Article N° 519
Contribution C.O.B. N° 705

OCEANOLOGICA ACTA 1981 - VOL. 4 - N° 2

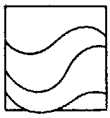

Gravity waves
Non-linearity
Statistics
Finite depth

Houle
Non-linéarité
Statistiques
Profondeur finie

# Non-linear deformation of sea-wave profiles in intermediate and shallow water

M. Arhan [a], R. O. Plaisted [b]

[a] Centre National pour l'Exploitation des Océans, Centre Océanologique de Bretagne, BP n° 337, 29273 Brest Cedex, France.

[b] Centro de Investigation Cientifica y de Education Superior de Ensenada (CICESE), APDO Postal 2732, Ensenada, Baja California, Mexique.

Received 1/10/80, in revised form 9/12/80, accepted 12/12/80.

## ABSTRACT

The present paper is a study of the nonlinear deformations of sea-wave profiles in intermediate (20 m depth) and shallow (4 m) water, based on wave staff and bottom pressure *in situ* measurements. The nonlinear deformations have been decomposed into two elementary classes: asymmetry with respect to the mean water surface. and asymmetry with respect to a vertical line passed through the wave crest.

The extend of the deformation of the first kind is estimated by computing the experimental statistical distributions of wave crest heights and through depths. These distributions are shown to deviate from the Rayleigh law (applicable to linear sea states), and are well fitted by a second order perturbation model deduced from the Stokes theory.

The second kind of nonlinear deformation was observed in shallow water only, and studied by a bi-spectral analysis: this kind of deformation may be interpreted in terms of a phase shift between first and second order components, and related to the phase of the bispectrum. It has been possible, applying this technique to the shallow water data set, to find anew the steepening of the wave front during its progression towards the breaking point.

*Oceanol. Acta*, 1981, **4**, 2, 107-115.

## RÉSUMÉ

### Déformations non linéaires du profil des vagues en eau de profondeur intermédiaire et en eau peu profonde

Les déformations non linéaires du profil des vagues en eau de profondeur intermédiaire (20 m) et en eau peu profonde (4 m) sont étudiées sur la base de mesures *in situ* effectuées par perches de houle et capteurs de pression. Ces déformations peuvent être classées en deux types : dissymétrie du profil par rapport au niveau moyen de la surface libre, et dissymétrie du profil par rapport à une verticale passant par la crête de la vague.

L'importance des déformations du premier type est évaluée en calculant les distributions statistiques expérimentales de hauteurs de crêtes et profondeurs de creux. Ces distributions, qui diffèrent sensiblement de la loi de Rayleigh (applicable aux états de mer linéaires), sont comparées, avec un bon accord, à un modèle de perturbation du second ordre déduit de la théorie de Stokes.

Le second type de déformation, observé en eau peu profonde seulement, est étudié par analyse bispectrale : cette déformation peut être interprétée en termes de déphasage entre composantes du premier et du second ordre, et est donc reliée à la phase du bispectre. On a pu suivre de cette façon, à partir des données en eau peu profonde, le raidissement du front des vagues à l'approche du point de déferlement.

## INTRODUCTION

The extend of non-linear deformations of real sea-waves is still subject to discussion. *In situ* measurements in intermediate and deep water, generally performed by wave-rider buoys, show very little non-linearity. On the other hand, numerous experiments carried out in wave tanks lead to highly non-linear wave profiles. When analysing the results, both kinds of studies may be suspected to deviate from reality; the former, because the sensor does not furnish an exactly Eulerian representation of the free surface displacement; the latter, due to the man-induced unidirectionality of wave tanks, which, for equal energy, must produce non-linearities higher than those present in multidirectional real wave fields.

An attempt to estimate correctly some non-linear parameters is made in the present study, based on two distinct sets of *in situ* measurements: weakly non-linear wave staff data from a 20 m depth site in the Gulf of Mexico, and highly non-linear bottom pressure data at a 3 to 4 m depth, on a beach in Brittany. The deviations from linearity are studied by a "zero-crossing" method and a bispectral analysis; results are compared in both cases to simple second order models.

The data are briefly presented in the first paragraph of the paper. Evidence is then given of non-linearity and its causes, by studying the variations of some typical deformation parameters as functions of individual wave heights and periods. It is well-known that the distribution functions of crests and troughs of linear sea-waves are correctly represented by the Rayleigh law. The deviations from this law are estimated and compared to a second order perturbation model deduced from the Stokes theory. The last paragraph deals with bispectral analysis and its application to the study of waves in shallow water; it is shown in particular that the phases of the bispectrum are related to the asymmetry of the wave profile with respect to the vertical axis drawn through the crest.

## PRESENTATION OF DATA

### Wave data from intermediate water

The data are part of the measurements performed at Exxon's Ocean Test Structure (OTS), at 20 m depth in the Gulf of Mexico, from December 1976 to June 1978. From this important data set, only the six channels (out of 96) corresponding to wave measurements were retained. The platform itself was equipped with five wave staffs, situated at each corner and at its center, and during the last winter, a Datawell waverider buoy was operated at a distance of a few hundred meters. Our study is restricted to the analysis of Storm Sea States periods ($H_{1/3} > 2.5$ m) for which the non-linearities are expected to be the highest. These selected periods were cut into 17 min. 4 sec. records, which corresponds to 2 048 points for the chosen digitizing rate (2 Hz). For each record a mean wave direction was estimated from the orbital velocities and wind measurements, and only the data from the wave staff facing the waves were retained. A total of 143 records have been selected in this way, which corresponds to about 40 hours in duration. The actual significant wave heights range between 2.5 and 4 m, and the spectral peak frequencies between 0.10 and 0.12 Hz.

### Shallow water data

The data were obtained during an experiment carried out by the Physical Oceanography Team of the Centre Océanologique de Bretagne, in January 1974, on the beach of La Palue, in the Crozon Peninsula, Brittany. It consists of bottom pressure measurements in a 4 m depth zone, where the severe Atlantic swell has come close to its breaking point. Twenty two 34 min. 8 sec. records were obtained, with significant wave heights ranging from 1.2 to 2 m, and spectral peak frequencies around 0.07 Hz.

## EVIDENCE OF NON-LINEARITY AND ITS CAUSES

### Previous studies of the shallow water data

Important non-linear features of these shallow water data have already been set in evidence in previous studies (Arhan, Gouriten, 1976; Cavanié, Ezraty, 1976).

– The histogram of bottom pressure variations was found to deviate considerably from a Gaussian law.

– Secondary peaks were present at harmonics of the main peak of the power spectra.

– The Rayleigh law, which in a linear context furnishes a correct representation of the probability density of wave heights, had to be replaced by a Weibull law, to take into account the saturation effect at the highest waves caused by the presence of the bottom.

### The third order moment

The normalized third order moment of a process furnishes a first indication of the importance of its non-linearities. The mean values of this parameter and of the fourth order moment, computed from both data sets and the waverider data, are summarized in the Table.

The $\bar{m}_3$ values reported in the first two lines of the Table reveal the presence of an important non-linearity in shallow water, and a lower but non negligible non-

*Table*

| Sensor | Water depth (m) | Number of records | $\bar{m}_3$ | $\bar{m}_4$ |
|---|---|---|---|---|
| Bottom pressure | 3 to 4 | 22 | 0.62 | 3.03 |
| Wave Staff | 20 | 141 | 0.148 | 3.02 |
| Wave Staff | 20 | 55 | 0.173 | 3.07 |
| Waverider buoy | 20 | 55 | 0.026 | 2.73 |

linearity in intermediate water. The values computed from the wave staff data are comparable to other experimental values given by Longuet-Higgins (1963). In the same paper, Longuet-Higgins derived theoretical limits for $\bar{m}_3$ – these were not tested here – and predicted that: $(\bar{m}_4 - 3) = \mathcal{O}(\bar{m}_3)^2$. This relation appears to be satisfied for both bottom pressure and wave staff data sets.

The two last lines allow a comparison between the third and fourth moments values estimated from the wave staff data and the waverider buoy data, for the same periods. It clearly appears that the latter sensor is unfit for detecting the non-linearities of sea waves. The reason for this must lie in the horizontal movements of the buoy with the surface water particles, from which two sources of error may be expected: a Doppler shift of the highest frequencies, and erroneous informations concerning possible phase links between different components. The Table shows that the fourth moment values are also underestimated by this sensor.

### Study of some deformation parameters

Following Kjeldsen and Myrhaug (1979) the non-linear deformations of sea-wave profiles are decomposed into two elementary classes:

– asymmetry with respect to the mean water surface; this deformation, characterized by an enhancement of crests and a flattening of troughs, is the only kind apparent in deep water, and leads, in the limit, to spilling breakers;

– asymmetry with respect to a vertical line passed through the crest, which affects essentially shallow water waves. The wave front steepens as it propagates shorewards, causing a plunging breaker at the end.

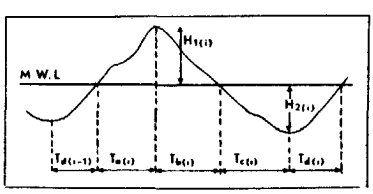


Figure 1
*The six zero-crossing parameters.* Les six paramètres *zero-crossing*.

Those two types of deformation have been detected by performing a "zero-crossing" analysis on both data sets. Six parameters have been computed for each individual wave (Fig. 1): $H_1$ and $H_2$ are respectively the crest height and trough depth with respect to the still water level. $T_a$, $T_b$, $T_c$, $T_d$ are the time lags separating the zero up or down crossings from the crests or troughs occurences. The ratios:

$$P_1(j) = (H_1(i) - H_2(i))/(H_1(i) + H_2(i)),$$

and

$$P_2(j) = (T_c(i) + T_d(i) - T_a(i) - T_b(i)) / (T_a(i) + T_b(i) + T_c(i) + T_d(i)),$$

characterize the asymmetry with respect to the still water level. $P_1$ compares the amplitudes of crest heights and trough depths, while $P_2$ compares the durations spend under and above the still water level. A third parameter $P_3$ measures the asymmetry of the wave with respect to a vertical axis in its crest:

$$P_3(j) = (T_b(i) + T_c(i) - T_a(i) - T_d(i-1)) / (T_d(i-1) + T_a(i) + T_b(i) + T_c(i)).$$

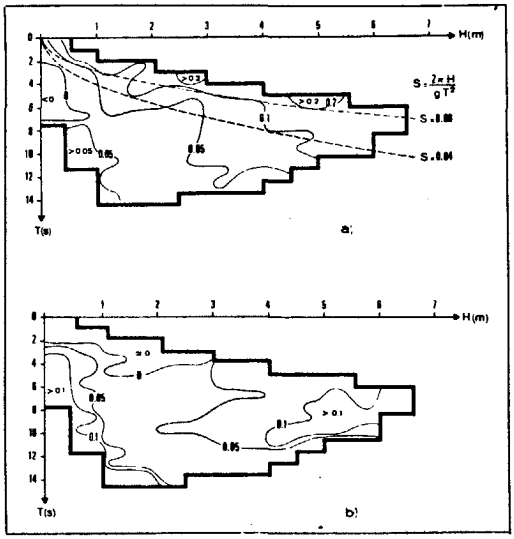


Figure 2
*Isocontours of the deformation parameters, in the plane* (H, T), *for the intermediate water case. a)* $\bar{P}_1$; *b)* $\bar{P}_2$.

Isolignes des paramètres de déformation dans le plan (H, T) pour les données en eau intermédiaire : *a)* $P_1$ ; *b)* $P_2$.

The subscript $(i)$ refers to the individual zero-up-crossing waves. The subscript $(j)$ refers to zero-up-crossing waves for $P_1$ and $P_2$, and to trough-to-trough waves (defined between two successive troughs) for $P_3$. The three parameters are expected to be zero on the average for linear sea-states and to be positive when non-linearities are present.

All waves of both data sets have been classified as a function of their height H and period T, and the mean values of $P_1$, $P_2$, $P_3$, noted $\bar{P}_1$, $\bar{P}_2$, $\bar{P}_3$, computed inside of elementary subsets $\Delta H \times \Delta T$. The variations of the $\bar{P}_i$ are reported on Figure 2, for intermediate water, and on Figure 3 for shallow water. The diagrams correspond to $\Delta H$ and $\Delta T$ values of 0.5 *m* and 1 *s* respectively, and only the $\bar{P}_i$ computed from 5 or more $P_i$ values were retained. The shallow water (H, T) domain appears to be limited in wave height at 3 m, that is about three quarters of the maximum water depth.

The dotted parabolic curves reported on Figure 2 *a* are lines of equal steepness, obtained from the deep water relation $s = 2\pi H/gT^2$. For low and moderate wave heights and periods, the $\bar{P}_1$ isocontours approximately follow those curves, which means that the wave steepness is the only parameter influencing $\bar{P}_1$ in this domain of the (H, T) plane. Both sets of curves diverge in the part of the

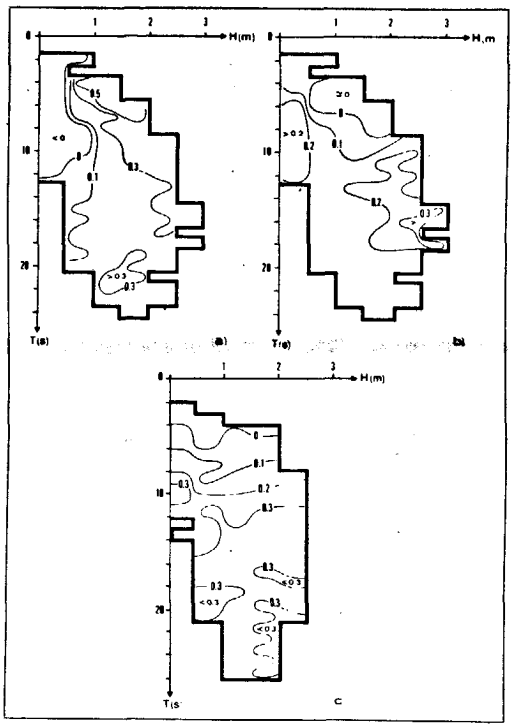

Figure 3

*Isocontours of the deformation parameters in the* (H, T) *plane, for the shallow water case. a)* $P_1$, *b)* $P_2$; *c)* $\overline{P}_3$.

Isolignes des paramètres de déformation dans le plan (H, T), pour les donnees en eau peu profonde : *a)* $P_1$ ; *b)* $P_2$ ; *c)* $P_3$.

diagram corresponding to the highest waves, the $\overline{P}_1$ values being then higher than would be expected from the steepness effect only. This increased non-linear deformation must be due to the effect of the bottom, all the more important as the wave period, hence the wave length, is high. These two basic effects – steepness effect and bottom effect – may also be clearly distinguished on the shallow water $\overline{P}_1$ diagram (Fig. 3 *a*). Although no parabolic isocontour is to be expected here, since the previous formula for the wave steepness is no longer applicable, the closed 0.3 isocontour in the lowest part of the diagram must clearly be attributed to bottom effects. The maximum values obtained for $\overline{P}_1$ are 0.25 for intermediate water and 0.40 for shallow water.

The $\overline{P}_2$ isocontours reported in the diagrams 2 *b* and 3 *b* reveal that this parameter is chiefly dependent on the wave height. But as was the case for $\overline{P}_1$, the influence of the bottom is effective for the highest waves. The highest $\overline{P}_2$ values are about 0.15 for intermediate water, and 0.30 for shallow water.

Perceptible deviations of $\overline{P}_3$ from zero were found in the shallow water case only. The diagram 3 *c* confirms that this kind of deformation – asymmetry with respect to a vertical axis at the crest – is directly related to the wave period (or wavelength), and thus must be attributed to bottom effects only. The maximum values found for $\overline{P}_3$ are about 0.4.

## ASYMMETRY WITH RESPECT TO THE MEAN WATER LEVEL. COMPARED DISTRIBUTIONS OF CREST HEIGHTS AND TROUGH DEPTHS

### Second order theoretical model

It is well known since the work of Cartwright and Longuet-Higgins (1956) that the statistical distribution of the crest heights (and trough depths) in a linear narrow banded wave field is well fitted by the Rayleigh law:

$$p(H)=\frac{H}{M_0}e^{-H^2/2M_0},$$

$M_0$ being the total energy of the wave field. When $M_0$ increases, there comes a moment when the non-linearities are to be taken into account. Retaining only the second order terms, it appears that some components must be present in the spectrum at twice the frequency of the initial spectral band, with a phase coupling between these components and those of the main peak. Assuming a sufficiently narrow spectrum, and considering the individual waves, these phase links between components cause an evolution towards profiles of the type "Stokes 2nd order", with enhanced crests and flat troughs. The Rayleigh law for the distribution of these variables is no longer valid, and has to be perturbed, as was the wave profile. This is the aim of the following model.

Each individual wave is assumed to have a "Stokes 2nd order" profile:

$$y_s=a\cos 2\pi\left(\frac{x}{L}-\frac{t}{T}\right)+Ba^2\cos 4\pi\left(\frac{x}{L}-\frac{t}{T}\right), \qquad (1)$$

with:

$$T^2=\frac{2\pi L}{g}\coth\left(\frac{2\pi d}{L}\right),$$

$$B=\frac{\pi}{L}\left(1+\frac{3}{2\,\mathrm{sh}^2(2\pi d/L)}\right)\coth\frac{2\pi d}{L}, \qquad (2)$$

where $d$ is the water depth, $g$ is the acceleration of gravity, L and T are the wave length and period respectively.

All the waves are assumed to have the same period. The amplitude, $a$, of the first order component, is supposed to be Rayleigh distributed, as would be the case for linear waves:

$$p(a)=\frac{a}{M_{01}}e^{-a^2/2M_{01}}, \qquad (3)$$

where $M_{01}$ is the part of the total energy $M_0$ to be attributed to first order components. The energy of the individual wave described in (1) is:

$$m_0=\frac{a^2}{2}+\frac{B^2a^4}{2},$$

from which:

$$M_{01} = \int_0^\infty \frac{a^2}{2} p(a)\, da.$$

In the same way, the total energy due to second order components is:

$$M_{02} = \int_0^\infty \frac{B^2 a^4}{2} p(a)\, da.$$

Resolving this integral reveals that:

$$M_{02} = 4 B^2 M_{01}^2.$$

Since:

$$M_0 = M_{01} + M_{02},$$

$M_{01}$ may be expressed in terms of $M_0$:

$$M_{01} = (-1 + \sqrt{1 + 16 M_0 B^2})/8B^2, \quad (4)$$

Given $M_0$, the distribution of the amplitude of the first order component, $a$, is now fully determined. The crest height and trough depth of the theoretical wave may be obtained from the same condensed relation:

$$H = a + \varepsilon B a^2, \quad (5)$$

with $\varepsilon = +1$ for crests, and $\varepsilon = -1$ for troughs.

The statistical distribution of H is then deduced from that of $a$:

$p(H)\, dH = p(a)\, da$.

Replacing $p(a)$ and $da$ in this equation by their expressions obtained from equations (2), (3), (4), (5), and normalizing H with respect to $\sqrt{M_0}$, leads to:

$$p(h) = \frac{\varepsilon\alpha(-1 + \sqrt{1+\varepsilon\alpha h})}{(-1+\sqrt{1+\alpha^2})\sqrt{1+\varepsilon\alpha h}} \times \exp\left\{-\frac{\varepsilon(-1+\sqrt{1+\varepsilon\alpha h})^2}{(-1+\sqrt{1+\alpha^2})}\right\}, \quad (6)$$

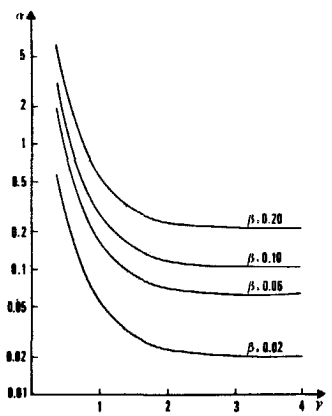


Figure 4

*Variations of the perturbation parameter α, as function of β and γ.*

Variations du paramètre de perturbation α, en fonction de β et γ.

with:

$$h = H/\sqrt{M_0},$$

$$\alpha = \beta\left(1 + \frac{3}{2\,\mathrm{sh}^2\gamma}\right)\coth\gamma, \quad (7)$$

$$\beta = 2k\sqrt{M_0},$$

$$\gamma = kd,$$

$$k = 2\pi/L.$$

The parameter β may be considered as a global steepness of the wave field, and γ, which relates the water depth to the wave length, characterizes the importance of bottom effects. Both kinds of non-linearities appear in the model through the unique perturbation parameter α. Figure 4 shows the variations of α as function of β and γ.

Developing the second member of equation (6) as function of α gives:

$$p(h) = he^{-h^2/2}\left[1 + \frac{\varepsilon h}{4}(h^2 - 3)\alpha + \alpha\mathcal{O}(\alpha)\right].$$

**Comparison of the model with weakly non-linear data from intermediate water**

A wave length characteristic of each 17 min. 4 sec. record of the OTS data was computed from the period $TH_{1/3}$ of the record, using the classical dispersion relation in intermediate water. $TH_{1/3}$ was chosen because of its stability with regards to high frequencies, and because only the highest third of crests and troughs were used to fit the model, as will be seen later. A value of α, called α Stokes, and noted $\alpha_s$, was computed for each record from equation (7), using $TH_{1/3}$, the standard deviation of the record, $\sqrt{M_0}$, and the constant water depth $d = 20{,}27$ m. The parameter $\alpha_s$ was found to vary in the range [0.13, 0.25]. The 143 records were distributed into ten groups as function of $\alpha_s$, so that more than 1 500 individual waves were present in each group. The cumulative probability of crest heights and trough depths was computed for each group, and the theoretical model defined by equation (6)

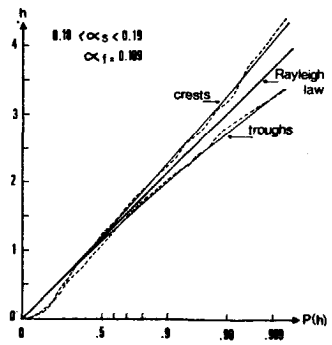


Figure 5

*Experimental and theoretical (fitted) distributions of crest heights and trough depths, in intermediate water.*

Distributions expérimentale et théorique (ajustée) des hauteurs de crêtes et profondeurs de creux, en eau intermédiaire.

fitted to each of these experimental distributions by using $\alpha$ as a fitting parameter. The fitting procedure was a least squares one, using the Rayleigh probability paper scales, and was performed on the highest third of crest heights and trough depths only, where the deviations from the Rayleigh law are the more pronounced.

The fitted value of $\alpha$ is noted $\alpha_f$. The goodness of fit obtained by this model is quite satisfactory, as may be seen from Figure 5, drawn for the subset of records corresponding to $0.18 < \alpha_s < 0.19$. The extend of the deviations from the Rayleigh law is shown to be more than 10 % for the highest values. It is also noticeable that the probability functions of crests and troughs begin to diverge for low values of these parameters ($H \simeq 0.5\sqrt{M_0}$).

Figure 6 compares the values of $\alpha_s$ and $\alpha_f$ for each group of records. The ratio $\alpha_f/\alpha_s$ ranges between 0.4 and 0.7 which means that the observed difference of behaviour between crests and troughs, and the observed deviations from the Rayleigh law are less than predicted by the Stokes second order theory. This result is to be attributed to the fact that a unidirectional model is being fitted to data from a multidirectional wave field: For a given value of the total energy, the non-linearities need not be as large when this energy is allowed to be spread in different directions.

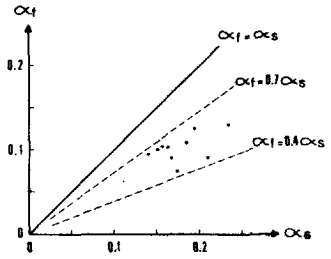


Figure 6

*Comparison between $\alpha_s$ and $\alpha_f$.*

Comparaison de $\alpha_s$ et $\alpha_f$.

This effect of directionality on non-linearity is the reason for the non-zero interval proposed by Longuet-Higgins (1963) for the variations of the coefficient of skewness. The present results are also consistent with those of Forristall *et al.* (1978) who showed that the wave-induced velocities are overpredicted by non-linear unidirectional wave theories, and those of Mitsuyasu *et al.* (1979), and Masuda *et al.* (1979) in their study of the dispersion relation of random gravity waves.

**Statistical distribution of crests and troughs for waves in shallow water**

Figure 7 shows the experimental cumulative probability curves of crest heights, trough depths, and half wave heights, for one of the shallow water records. The non-linear features already noticed for the OTS data appear to be more pronounced here. Those curves also reveal an effect of saturation of the three plotted parameters, due to

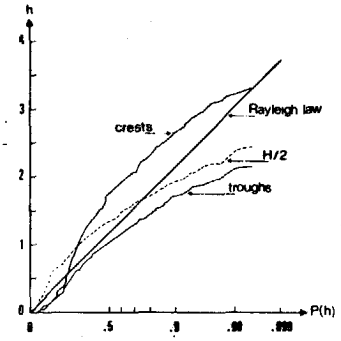


Figure 7

*Experimental distributions of crests, troughs, and half-heights of waves (H/2) in shallow water.*

Distributions expérimentales des crêtes, des creux et des demi-hauteurs de vagues (H/2), en eau peu profonde.

the shallowness of the water. Cavanié and Ezraty (1976) found that this latter effect is at the origin of a transformation of the wave height distribution towards a Weibull type law. It appears from Figure 7 that the crests and troughs probability functions are also affected.

The importance of non-linearities, and the presence of the saturation effect obviously prevent from correctly fitting to the shallow water experimental probabilities the perturbation model of equation (6).

## ASYMMETRY WITH RESPECT TO A VERTICAL LINE TROUGH THE CREST. BISPECTRAL ANALYSIS

Figure 8 reproduced from Arhan and Gouriten (1976), shows a portion of bottom pressure record in shallow water, with the corresponding power spectrum. The presence of a secondary spectral peak at twice the frequency of the main one, and the important skewness of

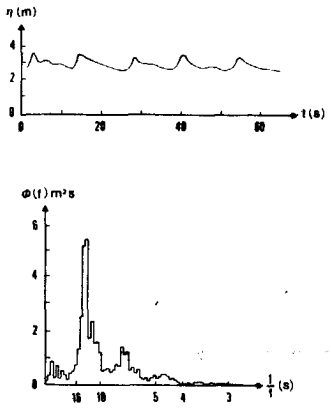


Figure 8

*Variations of bottom pressure in shallow water, and the corresponding power spectrum.*

Variations de pression au fond en eau peu profonde, et le spectre de puissance correspondant.

the profile, suggest that the components of the secondary peak are essentially forced waves resulting from 2nd order interactions of the main peak. Another characteristic feature of this portion of record, already set in evidence in the paragraph "study of some deformation parameters" is the asymmetry of shallow water wave profiles with respect to vertical axis through the crests. Figure 9 shows that this asymmetry may be interpreted as a consequence of a certain phase shift between the first and second order components. A way of studying this kind of deformation will then be to estimate this phase shift from wave records in shallow water. This is possible through bispectral analysis, and is the purpose of the present paragraph.

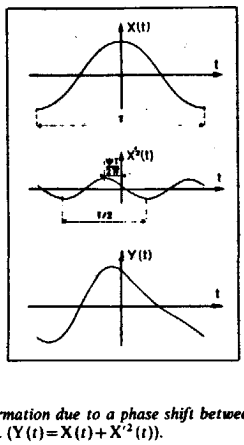


Figure 9

*Wave profile deformation due to a phase shift between first and second order components.* $(Y(t)=X(t)+X'^2(t))$.

Déformation du profil des vagues due à un déphasage entre composantes du premier et du second ordre :

$(Y(t)=X(t)+X'^2(t))$.

**Theoretical reminder on bispectra (Haubrich, 1965; Hinich, Clay, 1968)**

Bispectra were introduced in wave studies by Hasselmann *et al.* (1963), but they have not been widely used until recent years (Houmb, 1974; Liu, 1977). They furnish a measure of second order non-linear interactions, and must be related to the wave profile deformations studied in this work. Bispectral computations were carried out for both intermediate and shallow water data sets, but significant results were obtained in the latter case only.

The bispectrum of a stationnary random process $X(t)$ is defined as the two dimensional Fourier transform of the second order covariance:

$$B(f_1,f_2)=\iint_{-\infty}^{\infty} R(\tau_1,\tau_2)e^{-2\pi i(f_1\tau_1+f_2\tau_2)}d\tau_1 d\tau_2, \qquad (8)$$

with:

$$R(\tau_1,\tau_2)=E[X(t)X(t+\tau_1)X(t+\tau_2)].$$

Since all third moments of a Gaussian process are zero, any deviation from Normality will be detected by a non-zero value of the bispectrum. As is currently done for power spectra (Hinich, Clay, 1968) the order of operations in formula (8)—covariance computation, then Fourier transform—may be inverted so that the Fourier transform is carried out first. This method allows rapid computations of bispectra from finite duration records:

$$B_{jk}=E[X_jX_kX^*_{j+k}], \qquad (9)$$

where the subscripts are the number of the harmonics, and the Fourier transform of the signal, $X_j$, is defined from:

$$X(t)=\sum_{j=-\infty}^{+\infty} X_j e^{i\omega_j t}, \qquad X_{-j}=X^*_j, \quad \omega_j=2\pi j/T.$$

$X^*_j$ denotes the complex conjugate of $X_j$.

The expectancy in (9) is taken over a great number of finite duration records.

Let each $X_j$ be written as function of its amplitude and phase:

$$X_j=|X_j|e^{i\theta_j},$$

then:

$$B_{jk}=E[X_{jk}e^{i\theta_{jk}}],$$

with:

$$X_{jk}=|X_j|.|X_k|.|X_{j+k}|,$$
$$\theta_{jk}=\theta_j+\theta_k-\theta_{j+k}.$$

Assuming that the amplitudes of the components are known exactly:

$$B_{jk}\doteq X_{jk}E[e^{i\theta_{jk}}],$$

or:

$$B_{jk}=X_{jk}\{E[\cos\theta_{jk}]+iE[\sin\theta_{jk}]\}. \qquad (10)$$

This formulation leads to an interpretation of bispectra in terms of phase links between components. If $X(t)$ is a linear Gaussian process, the $\theta_j$'s are uniformly distributed over $[0, 2\pi]$, and mutually independent. The angle $\theta_{jk}$ is then also uniformly distributed over $[0, 2\pi]$, and the bispectrum is zero. On the other hand, if some permanent non-linear phase links exist between the components, resulting in a non-uniform distribution of $\theta_{jk}$, the bispectrum is different from zero.

A handy form for bispectra, which has been used in this work, is obtained by expressing them in terms of their normalized squared amplitude, or bicoherence, and phase:

$$R^2_{jk}=\frac{|E[X_jX_kX^*_{j+k}]|^2}{E[X_jX^*_j]E[X_kX^*_k]E[X_{j+k}X^*_{j+k}]},$$

$$\varphi_{jk}=\text{arctg}\left\{\frac{Im[B_{jk}]}{\mathcal{R}e[B_{jk}]}\right\}.$$

### A second order model for waves in shallow water

The comments on Figure 8 made at the beginning of this paragraph, concerning the phase shift between first and second order components, and the narrowness of the main peak of the spectrum, suggest representing the reported shallow water signal by the following model:

$$Y(t)=X(t)+X'^2(t), \tag{11}$$

where $X(t)$ and $X'(t)$ are narrow banded linear processes, with a constant phase shift between their components. This may be written, in terms of their Fourier transforms:

$$X_j=|X_j|e^{i\theta_j},$$
$$X'_j=|X'_j|e^{i\theta'_j}, \quad \text{with} \quad \theta'_j=\theta_j+\psi_j,$$

with $X_j$ and $X'_j$ different from zero in the narrow frequency bands $[j_1, j_2]$ and $[-j_2, -j_1]$ only. $X'(t)$ may be considered as the output of a linear filter applied to $X(t)$. In the following we restrict ourselves to the simplified case of single band spectra for $X(t)$ and $X'(t)$ ($j_1=j_2=l$). This leads to a simple expression and an easy interpretation of the bispectrum of $Y(t)$.

The Fourier transform of $Y(t)$ is readily deduced from (11):

$$Y_i=X_i+\sum_{j=-\infty}^{+\infty} X'_j X'_{j-i}. \tag{12}$$

Introducing in (12) the $X'_i$'s of the single banded model leads to:

$$Y_i=0,$$

except for:

$$Y_0=2X'_l X'^*_l,$$
$$Y_{\pm l}=X_{\pm l},$$
$$Y_{\pm 2l}=X'_{\pm l}X'_{\pm l}.$$

Using these relations in $B_{pq}=Y_p\,Y_q\,Y^*_{p+q}$ shows that only $B_{00}$, $B_{0l}$, $B_{0,2l}$ and $B_{ll}$ are different from zero. Now considering the phases, it appears that only $B_{ll}$ has a non-zero phase:

$$B_{ll}=Y_l Y_l Y^*_{2l},$$
$$B_{ll}=X_l X_l X'^*_l X'^*_l.$$

From this latter expression, the phase of $B_{ll}$, noted $\varphi_{ll}$, is obtained:

$$\varphi_{ll}=-2\psi_l. \tag{13}$$

Thus assuming the preceding model is a reasonable representation of reality, bispectral computations should furnish a measure of the phase shift between first and second order components. The usually observed deformations of shallow water wave profiles – forward side steeper than backside – indicate a phase advance of the second order component ($\psi>0$, $\varphi<0$). It is noticeable that a phase delay of these forced second order oscillations would be explained by the damping effect of the bottom. The observed phase advance must then be attributed to another cause, probably the bottom slope.

### Comparison with experiment

The bicoherences and bispectral phases of the 22 shallow water records were computed in the following way. Each 34 min. 8 sec. record was digitized at a rate of 1 Hz and divided into thirty two 64 sec. long non-overlapping groups, and the corresponding thirty one half-overlapping groups. The expectancy appearing in equation (9) was estimated by averaging over those 63 groups. Retaining the half-overlapping groups has the advantage of increasing by a factor of about 1.4 the number of degrees of freedom $\nu$ of spectral estimates (Cooley *et al.*, 1967), leading to $\nu=90$. Assuming a true zero value of the bispectrum, Haubrich (1965), showed that the 95% confidence interval of the bicoherence was $6/\nu$. In the present case, this limit will then be equal to 0.067. Figure 10 shows the bicoherence isocontours and the corresponding power spectrum of a record. The 95% confidence limit is clearly exceeded, revealing important non-linear interactions between components of the main peak and their harmonics.

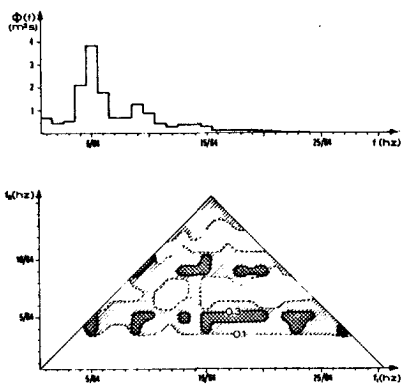

Figure 10

*Power spectrum and bicoherence computed from data in shallow water.*

Spectre de puissance et bicohérence d'un enregistrement en eau peu profonde.

The phases of the bispectra were found negative over the areas of significant bicoherence, in particular at the position of the peak ($\varphi_{ll}$), which confirms a phase advance of second order components [equation (13)]. The steepening of the forward side of waves as they progress shorewards may be interpreted as an increase of $|\varphi_{ll}|$. This phase value was examined for each bispectrum, and is reported on Figure 11 as a function of $d/\lambda$, where $d$ is the water depth and $\lambda$ a wavelength characteristic of the record, computed from the spectral peak frequency and the deep water dispersion relation. The variations of $d$, due to the tide effect, and those of $\lambda$ resulting from the spectral evolution, cause $d/\lambda$ to vary, and simulate the wave shoaling. Figure 11 is a confirmation of the expected trend, with a reasonable scattering of the 22 reported points. The highest values of the phase advance, deduced from this figure, are about 40° ($\psi_l=|\varphi_{ll}|/2$). It must be kept in mind, however, when analysing this figure, that the $\varphi_{ll}$ estimates are

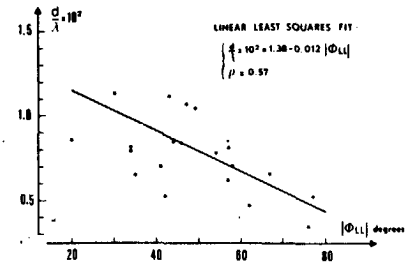


Figure 11
*Phase of the bispectrum ($\varphi_{II}$) as function of $d/\lambda$.*

Phase du bispectre ($\varphi_{II}$) en fonction de $d/\lambda$.

dependent – as is the estimated peak level of a narrow banded power spectrum – on the frequency resolution, and thus may be slightly biased.

## CONCLUSIONS

An asymmetry with respect to the mean water level is the only significant non-linear deformation found in the intermediate water case. Except for the highest waves, where a bottom effect is perceptible, this kind of deformation is chiefly dependent on the wave steepness. A second order model for the distributions of crest heights and trough depths was shown to explain, but to overpredict this deformation. This overprediction must be attributed to the uni-directionality of the theory, and leads to the recommendation that the angular dispersion of energy in real wave fields be estimated and taken into account in such models, prior to considering higher order non-linear terms.

This kind of deformation is more pronounced in shallow water, although partly compensated, for the highest crests and lowest troughs, by a saturation effect due to the bottom.

Another kind of non-linear wave profile deformation is observed in shallow water only. It consists in an asymmetry with respect to a vertical line passed through the crest, and can be interpreted in terms of a phase shift between first and second order components. The analysis of bispectra, and in particular of their phases, appears as a way of studying this kind of deformation.


## Acknowledgements

The present work was done on behalf of the Bureau Veritas who participated in Exxon's Ocean Test Structure program. The intermediate water data were put at our disposal by the Bureau Veritas. We also wish to acknowledge the many suggestions and remarks made by A. Cavanié during this work.


## REFERENCES


**Arhan M., Gouriten Y.**, 1976. Relations entre les variations de pression au fond et les courants particulaires dans la houle côtière proche du déferlement, *Ann. Hydrog.*, série 5, **4**, 1.

**Cartwright D. E., Longuet-Higgins M. S.**, 1956. The statistical distribution of the maxima of a random function, *Proc. R. Soc.*, ser. A, **237**, 212-232.

**Cavanie A., Ezraty R.**, 1976. Étude statistique de la houle littorale proche du déferlement, *Ann. Hydrogr.*, sér. 5, **4**, 1.

**Cooley J. W., Lewis P. A. W., Welch P. D.**, 1967. The fast Fourier Transform algorithm and its applications, IBM Watson Research Center, Yorktown Heights, New York, Res. Pap. RC, 1743.

**Forristall G. Z., Ward E. G., Cardone V. J., Borgman L. E.**, 1978. The directional spectra and kinematics of surface gravity waves in tropical storm Delia, *J. Phys. Oceanogr.*, **8**, 5, 888-909.

**Hasselmann K., Munk W., MacDonald D. G.**, 1963. Bispectra of ocean waves, in: *Time series analysis*, Rosenblatt Wiley, New York, 125.

**Haubrich R. A.**, 1965. Earth noise, 5 to 500 millicycles per second. 1) Spectral stationarity, normality and non-linearity, *J. Geophys. Res.*, **70**, 6

**Hinich M. J., Clay C. S.**, 1968. The application of the discrete Fourier Transform in the estimation of power spectra, coherence and bispectra of geophysical data, *Rev. Geophys.*, **6**, 3.

**Houmb O. G.**, 1974. Spectra and bispectra of ocean waves, 1974 Coastal Engineering Conference.

**Kjeldsen S. P., Myrhaug D.**, 1979. Formation of wave groups and distributions of parameters for wave asymmetry from "Ships in Rough Seas", Part 4, Norwegian Hydrodynamic Laboratories Report.

**Liu P. C.**, 1977. Higher order spectra and stationarity of wind waves, Fifth conference on probability and statistics, Las Vegas.

**Longuet-Higgins M. S.**, 1963. The effects of non-linearities on statistical distributions in the theory of sea-waves, *J. Fluid Mech.*, **17**, 3, 459-480.

**Masuda A., Kuo Y., Mitsuyasu H.**, 1979. On the dispersion relation of random gravity waves. Part 1, Theoretical framework, *J. Fluid Mech.*, **92**, 4, 717-730.

**Mitsuyasu H., Kuo Y., Masuda A.**, 1979. On the dispersion relation of random gravity waves, Part 2, an experiment, *J. Fluid Mech.*, **92**, 4, 731-749.